

Measurement of the Lifetime of the B_c^\pm Meson in the Semileptonic Decay Channel

V. M. Abazov,³⁶ B. Abbott,⁷⁵ M. Abolins,⁶⁵ B. S. Acharya,²⁹ M. Adams,⁵¹ T. Adams,⁴⁹ E. Aguilo,⁶ S. H. Ahn,³¹ M. Ahsan,⁵⁹ G. D. Alexeev,³⁶ G. Alkhazov,⁴⁰ A. Alton,^{64,*} G. Alverson,⁶³ G. A. Alves,² M. Anastasoie,³⁵ L. S. Ancu,³⁵ T. Andeen,⁵³ S. Anderson,⁴⁵ B. Andrieu,¹⁷ M. S. Anzels,⁵³ M. Aoki,⁵⁰ Y. Arnoud,¹⁴ M. Arov,⁶⁰ M. Arthaud,¹⁸ A. Askew,⁴⁹ B. Åsman,⁴¹ A. C. S. Assis Jesus,³ O. Atramentov,⁴⁹ C. Avila,⁸ F. Badaud,¹³ A. Baden,⁶¹ L. Bagby,⁵⁰ B. Baldin,⁵⁰ D. V. Bandurin,⁵⁹ P. Banerjee,²⁹ S. Banerjee,²⁹ E. Barberis,⁶³ A.-F. Barfuss,¹⁵ P. Bargassa,⁸⁰ P. Baringer,⁵⁸ J. Barreto,² J. F. Bartlett,⁵⁰ U. Bassler,¹⁸ D. Bauer,⁴³ S. Beale,⁶ A. Bean,⁵⁸ M. Begalli,³ M. Begel,⁷³ C. Belanger-Champagne,⁴¹ L. Bellantoni,⁵⁰ A. Bellavance,⁵⁰ J. A. Benitez,⁶⁵ S. B. Beri,²⁷ G. Bernardi,¹⁷ R. Bernhard,²³ I. Bertram,⁴² M. Besançon,¹⁸ R. Beuselinck,⁴³ V. A. Bezzubov,³⁹ P. C. Bhat,⁵⁰ V. Bhatnagar,²⁷ C. Biscarat,²⁰ G. Blazey,⁵² F. Blekman,⁴³ S. Blessing,⁴⁹ D. Bloch,¹⁹ K. Bloom,⁶⁷ A. Boehnlein,⁵⁰ D. Boline,⁶² T. A. Bolton,⁵⁹ E. E. Boos,³⁸ G. Borissov,⁴² T. Bose,⁷⁷ A. Brandt,⁷⁸ R. Brock,⁶⁵ G. Brooijmans,⁷⁰ A. Bross,⁵⁰ D. Brown,⁸¹ N. J. Buchanan,⁴⁹ D. Buchholz,⁵³ M. Buehler,⁸¹ V. Buescher,²² V. Bunichev,³⁸ S. Burdin,^{42,†} S. Burke,⁴⁵ T. H. Burnett,⁸² C. P. Buszello,⁴³ J. M. Butler,⁶² P. Calfayan,²⁵ S. Calvet,¹⁶ J. Cammin,⁷¹ W. Carvalho,³ B. C. K. Casey,⁵⁰ H. Castilla-Valdez,³³ S. Chakrabarti,¹⁸ D. Chakraborty,⁵² K. Chan,⁶ K. M. Chan,⁵⁵ A. Chandra,⁴⁸ F. Charles,^{19,**} E. Cheu,⁴⁵ F. Chevallier,¹⁴ D. K. Cho,⁶² S. Choi,³² B. Choudhary,²⁸ L. Christofek,⁷⁷ T. Christoudias,⁴³ S. Cihangir,⁵⁰ D. Claes,⁶⁷ J. Clutter,⁵⁸ M. Cooke,⁸⁰ W. E. Cooper,⁵⁰ M. Corcoran,⁸⁰ F. Couderc,¹⁸ M.-C. Cousinou,¹⁵ S. Crépe-Renaudin,¹⁴ D. Cutts,⁷⁷ M. Ćwiok,³⁰ H. da Motta,² A. Das,⁴⁵ G. Davies,⁴³ K. De,⁷⁸ S. J. de Jong,³⁵ E. De La Cruz-Burelo,⁶⁴ C. De Oliveira Martins,³ J. D. Degenhardt,⁶⁴ F. Déliot,¹⁸ M. Demarteau,⁵⁰ R. Demina,⁷¹ D. Denisov,⁵⁰ S. P. Denisov,³⁹ S. Desai,⁵⁰ H. T. Diehl,⁵⁰ M. Diesburg,⁵⁰ A. Dominguez,⁶⁷ H. Dong,⁷² L. V. Dudko,³⁸ L. Dufлот,¹⁶ S. R. Dugad,²⁹ D. Duggan,⁴⁹ A. Duperrin,¹⁵ J. Dyer,⁶⁵ A. Dyshkant,⁵² M. Eads,⁶⁷ D. Edmunds,⁶⁵ J. Ellison,⁴⁸ V. D. Elvira,⁵⁰ Y. Enari,⁷⁷ S. Eno,⁶¹ P. Ermolov,³⁸ H. Evans,⁵⁴ A. Evdokimov,⁷³ V. N. Evdokimov,³⁹ A. V. Ferapontov,⁵⁹ T. Ferbel,⁷¹ F. Fiedler,²⁴ F. Filthaut,³⁵ W. Fisher,⁵⁰ H. E. Fisk,⁵⁰ M. Fortner,⁵² H. Fox,⁴² S. Fu,⁵⁰ S. Fuess,⁵⁰ T. Gadfort,⁷⁰ C. F. Galea,³⁵ E. Gallas,⁵⁰ C. Garcia,⁷¹ A. Garcia-Bellido,⁸² V. Gavrilov,³⁷ P. Gay,¹³ W. Geist,¹⁹ D. Gelé,¹⁹ C. E. Gerber,⁵¹ Y. Gershtein,⁴⁹ D. Gillberg,⁶ G. Ginther,⁷¹ N. Gollub,⁴¹ B. Gómez,⁸ A. Goussiou,⁸² P. D. Grannis,⁷² H. Greenlee,⁵⁰ Z. D. Greenwood,⁶⁰ E. M. Gregores,⁴ G. Grenier,²⁰ Ph. Gris,¹³ J.-F. Grivaz,¹⁶ A. Grohsjean,²⁵ S. Grünendahl,⁵⁰ M. W. Grünewald,³⁰ F. Guo,⁷² J. Guo,⁷² G. Gutierrez,⁵⁰ P. Gutierrez,⁷⁵ A. Haas,⁷⁰ N. J. Hadley,⁶¹ P. Haefner,²⁵ S. Hagopian,⁴⁹ J. Haley,⁶⁸ I. Hall,⁶⁵ R. E. Hall,⁴⁷ L. Han,⁷ K. Harder,⁴⁴ A. Harel,⁷¹ J. M. Hauptman,⁵⁷ R. Hauser,⁶⁵ J. Hays,⁴³ T. Hebbeker,²¹ D. Hedin,⁵² J. G. Hegeman,³⁴ A. P. Heinson,⁴⁸ U. Heintz,⁶² C. Hensel,^{22,§} K. Herner,⁷² G. Hesketh,⁶³ M. D. Hildreth,⁵⁵ R. Hirosky,⁸¹ J. D. Hobbs,⁷² B. Hoeneisen,¹² H. Hoeth,²⁶ M. Hohlfeld,²² S. J. Hong,³¹ S. Hossain,⁷⁵ P. Houben,³⁴ Y. Hu,⁷² Z. Hubacek,¹⁰ V. Hynek,⁹ I. Iashvili,⁶⁹ R. Illingworth,⁵⁰ A. S. Ito,⁵⁰ S. Jabeen,⁶² M. Jaffré,¹⁶ S. Jain,⁷⁵ K. Jakobs,²³ C. Jarvis,⁶¹ R. Jesik,⁴³ K. Johns,⁴⁵ C. Johnson,⁷⁰ M. Johnson,⁵⁰ A. Jonckheere,⁵⁰ P. Jonsson,⁴³ A. Juste,⁵⁰ E. Kajfasz,¹⁵ J. M. Kalk,⁶⁰ D. Karmanov,³⁸ P. A. Kasper,⁵⁰ I. Katsanos,⁷⁰ D. Kau,⁴⁹ V. Kaushik,⁷⁸ R. Kehoe,⁷⁹ S. Kermiche,¹⁵ N. Khalatyan,⁵⁰ A. Khanov,⁷⁶ A. Kharchilava,⁶⁹ Y. M. Kharzheev,³⁶ D. Khatidze,⁷⁰ T. J. Kim,³¹ M. H. Kirby,⁵³ M. Kirsch,²¹ B. Klima,⁵⁰ J. M. Kohli,²⁷ J.-P. Konrath,²³ A. V. Kozelov,³⁹ J. Kraus,⁶⁵ D. Krop,⁵⁴ T. Kuhl,²⁴ A. Kumar,⁶⁹ A. Kupco,¹¹ T. Kurča,²⁰ V. A. Kuzmin,³⁸ J. Kvita,⁹ F. Lacroix,¹³ D. Lam,⁵⁵ S. Lammers,⁷⁰ G. Landsberg,⁷⁷ P. Lebrun,²⁰ W. M. Lee,⁵⁰ A. Leflat,³⁸ J. Lellouch,¹⁷ J. Leveque,⁴⁵ J. Li,⁷⁸ L. Li,⁴⁸ Q. Z. Li,⁵⁰ S. M. Lietti,⁵ J. G. R. Lima,⁵² D. Lincoln,⁵⁰ J. Linnemann,⁶⁵ V. V. Lipaev,³⁹ R. Lipton,⁵⁰ Y. Liu,⁷ Z. Liu,⁶ A. Lobodenko,⁴⁰ M. Lokajicek,¹¹ P. Love,⁴² H. J. Lubatti,⁸² R. Luna,³ A. L. Lyon,⁵⁰ A. K. A. Maciel,² D. Mackin,⁸⁰ R. J. Madaras,⁴⁶ P. Mättig,²⁶ C. Magass,²¹ A. Magerkurth,⁶⁴ P. K. Mal,⁸² H. B. Malbouisson,³ S. Malik,⁶⁷ V. L. Malyshev,³⁶ H. S. Mao,⁵⁰ Y. Maravin,⁵⁹ B. Martin,¹⁴ R. McCarthy,⁷² A. Melnitchouk,⁶⁶ L. Mendoza,⁸ P. G. Mercadante,⁵ M. Merkin,³⁸ K. W. Merritt,⁵⁰ A. Meyer,²¹ J. Meyer,^{22,§} T. Millet,²⁰ J. Mitrevski,⁷⁰ R. K. Mommsen,⁴⁴ N. K. Mondal,²⁹ R. W. Moore,⁶ T. Moulik,⁵⁸ G. S. Muanza,²⁰ M. Mulhearn,⁷⁰ O. Mundal,²² L. Mundim,³ E. Nagy,¹⁵ M. Naimuddin,⁵⁰ M. Narain,⁷⁷ N. A. Naumann,³⁵ H. A. Neal,⁶⁴ J. P. Negret,⁸ P. Neustroev,⁴⁰ H. Nilsen,²³ H. Nogima,³ S. F. Novaes,⁵ T. Nunnemann,²⁵ V. O'Dell,⁵⁰ D. C. O'Neil,⁶ G. Obrant,⁴⁰ C. Ochando,¹⁶ D. Onoprienko,⁵⁹ N. Oshima,⁵⁰ N. Osman,⁴³ J. Osta,⁵⁵ R. Otec,¹⁰ G. J. Otero y Garzón,⁵⁰ M. Owen,⁴⁴ P. Padley,⁸⁰ M. Pangilinan,⁷⁷ N. Parashar,⁵⁶ S.-J. Park,^{22,§} S. K. Park,³¹ J. Parsons,⁷⁰ R. Partridge,⁷⁷ N. Parua,⁵⁴ A. Patwa,⁷³ G. Pawloski,⁸⁰ B. Penning,²³ M. Perfilov,³⁸ K. Peters,⁴⁴ Y. Peters,²⁶ P. Pétroff,¹⁶ M. Petteni,⁴³ R. Piegaia,¹ J. Piper,⁶⁵ M.-A. Pleier,²² P. L. M. Podesta-Lerma,^{33,‡} V. M. Podstavkov,⁵⁰ Y. Pogorelov,⁵⁵ M.-E. Pol,² P. Polozov,³⁷ B. G. Pope,⁶⁵ A. V. Popov,³⁹ C. Potter,⁶ W. L. Prado da Silva,³ H. B. Prosper,⁴⁹ S. Protopopescu,⁷³ J. Qian,⁶⁴ A. Quadt,^{22,§} B. Quinn,⁶⁶ A. Rakitine,⁴² M. S. Rangel,² K. Ranjan,²⁸ P. N. Ratoff,⁴² P. Renkel,⁷⁹ S. Reucroft,⁶³ P. Rich,⁴⁴ J. Rieger,⁵⁴ M. Rijssenbeek,⁷² I. Ripp-Baudot,¹⁹ F. Rizatdinova,⁷⁶ S. Robinson,⁴³ R. F. Rodrigues,³

M. Rominsky,⁷⁵ C. Royon,¹⁸ P. Rubinov,⁵⁰ R. Ruchti,⁵⁵ G. Safronov,³⁷ G. Sajot,¹⁴ A. Sánchez-Hernández,³³
M. P. Sanders,¹⁷ B. Sanghi,⁵⁰ A. Santoro,³ G. Savage,⁵⁰ L. Sawyer,⁶⁰ T. Scanlon,⁴³ D. Schaile,²⁵ R. D. Schamberger,⁷²
Y. Scheglov,⁴⁰ H. Schellman,⁵³ T. Schliephake,²⁶ C. Schwanenberger,⁴⁴ A. Schwartzman,⁶⁸ R. Schwienhorst,⁶⁵
J. Sekaric,⁴⁹ H. Severini,⁷⁵ E. Shabalina,⁵¹ M. Shamim,⁵⁹ V. Shary,¹⁸ A. A. Shchukin,³⁹ R. K. Shivpuri,²⁸ V. Siccardi,¹⁹
V. Simak,¹⁰ V. Sirotenko,⁵⁰ P. Skubic,⁷⁵ P. Slattery,⁷¹ D. Smirnov,⁵⁵ G. R. Snow,⁶⁷ J. Snow,⁷⁴ S. Snyder,⁷³
S. Söldner-Rembold,⁴⁴ L. Sonnenschein,¹⁷ A. Sopczak,⁴² M. Sosebee,⁷⁸ K. Soustruznik,⁹ B. Spurlock,⁷⁸ J. Stark,¹⁴
J. Steele,⁶⁰ V. Stolin,³⁷ D. A. Stoyanova,³⁹ J. Strandberg,⁶⁴ S. Strandberg,⁴¹ M. A. Strang,⁶⁹ E. Strauss,⁷² M. Strauss,⁷⁵
R. Ströhmer,²⁵ D. Strom,⁵³ L. Stutte,⁵⁰ S. Sumowidagdo,⁴⁹ P. Svoisky,⁵⁵ A. Sznajder,³ P. Tamburello,⁴⁵ A. Tanasijczuk,¹
W. Taylor,⁶ J. Temple,⁴⁵ B. Tiller,²⁵ F. Tissandier,¹³ M. Titov,¹⁸ V. V. Tokmenin,³⁶ T. Toole,⁶¹ I. Torchiani,²³ T. Trefzger,²⁴
D. Tsybychev,⁷² B. Tuchming,¹⁸ C. Tully,⁶⁸ P. M. Tuts,⁷⁰ R. Unalan,⁶⁵ L. Uvarov,⁴⁰ S. Uvarov,⁴⁰ S. Uzunyan,⁵² B. Vachon,⁶
P. J. van den Berg,³⁴ R. Van Kooten,⁵⁴ W. M. van Leeuwen,³⁴ N. Varelas,⁵¹ E. W. Varnes,⁴⁵ I. A. Vasilyev,³⁹ M. Vaupel,²⁶
P. Verdier,²⁰ L. S. Vertogradov,³⁶ M. Verzocchi,⁵⁰ F. Villeneuve-Seguiet,⁴³ P. Vint,⁴³ P. Vokac,¹⁰ E. Von Toerne,⁵⁹
M. Voutilainen,^{68,||} R. Wagner,⁶⁸ H. D. Wahl,⁴⁹ L. Wang,⁶¹ M. H. L. S. Wang,⁵⁰ J. Warchol,⁵⁵ G. Watts,⁸² M. Wayne,⁵⁵
G. Weber,²⁴ M. Weber,⁵⁰ L. Welty-Rieger,⁵⁴ A. Wenger,^{23,¶} N. Wermes,²² M. Wetstein,⁶¹ A. White,⁷⁸ D. Wicke,²⁶
G. W. Wilson,⁵⁸ S. J. Wimpenny,⁴⁸ M. Wobisch,⁶⁰ D. R. Wood,⁶³ T. R. Wyatt,⁴⁴ Y. Xie,⁷⁷ S. Yacoub,⁵³ R. Yamada,⁵⁰
M. Yan,⁶¹ T. Yasuda,⁵⁰ Y. A. Yatsunenko,³⁶ K. Yip,⁷³ H. D. Yoo,⁷⁷ S. W. Youn,⁵³ J. Yu,⁷⁸ C. Zeitnitz,²⁶ T. Zhao,⁸²
B. Zhou,⁶⁴ J. Zhu,⁷² M. Zielinski,⁷¹ D. Zieminska,⁵⁴ A. Zieminski,^{54,**} L. Zivkovic,⁷⁰ V. Zutshi,⁵² and E. G. Zverev³⁸

(D0 Collaboration)

¹Universidad de Buenos Aires, Buenos Aires, Argentina²LAFEX, Centro Brasileiro de Pesquisas Físicas, Rio de Janeiro, Brazil³Universidade do Estado do Rio de Janeiro, Rio de Janeiro, Brazil⁴Universidade Federal do ABC, Santo André, Brazil⁵Instituto de Física Teórica, Universidade Estadual Paulista, São Paulo, Brazil⁶University of Alberta, Edmonton, Alberta, Canada,

Simon Fraser University, Burnaby, British Columbia, Canada,

York University, Toronto, Ontario, Canada,

and McGill University, Montreal, Quebec, Canada

⁷University of Science and Technology of China, Hefei, People's Republic of China⁸Universidad de los Andes, Bogotá, Colombia⁹Center for Particle Physics, Charles University, Prague, Czech Republic¹⁰Czech Technical University, Prague, Czech Republic¹¹Center for Particle Physics, Institute of Physics, Academy of Sciences of the Czech Republic, Prague, Czech Republic¹²Universidad San Francisco de Quito, Quito, Ecuador¹³LPC, Univ Blaise Pascal, CNRS/IN2P3, Clermont, France¹⁴LPSC, Université Joseph Fourier Grenoble 1, CNRS/IN2P3, Institut National Polytechnique de Grenoble, Grenoble, France¹⁵CPPM, Aix-Marseille Université, CNRS/IN2P3, Marseille, France¹⁶LAL, Univ Paris-Sud, IN2P3/CNRS, Orsay, France¹⁷LPNHE, IN2P3/CNRS, Universités Paris VI and VII, Paris, France¹⁸DAPNIA/Service de Physique des Particules, CEA, Saclay, France¹⁹IPHC, Université Louis Pasteur et Université de Haute Alsace, CNRS/IN2P3, Strasbourg, France²⁰IPNL, Université Lyon 1, CNRS/IN2P3, Villeurbanne, France, and Université de Lyon, Lyon, France²¹III. Physikalisches Institut A, RWTH Aachen, Aachen, Germany²²Physikalisches Institut, Universität Bonn, Bonn, Germany²³Physikalisches Institut, Universität Freiburg, Freiburg, Germany²⁴Institut für Physik, Universität Mainz, Mainz, Germany²⁵Ludwig-Maximilians-Universität München, München, Germany²⁶Fachbereich Physik, University of Wuppertal, Wuppertal, Germany²⁷Panjab University, Chandigarh, India²⁸Delhi University, Delhi, India²⁹Tata Institute of Fundamental Research, Mumbai, India³⁰University College Dublin, Dublin, Ireland³¹Korea Detector Laboratory, Korea University, Seoul, Korea³²SungKyunKwan University, Suwon, Korea³³CINVESTAV, Mexico City, Mexico³⁴FOM-Institute NIKHEF and University of Amsterdam/NIKHEF, Amsterdam, The Netherlands

- ³⁵Radboud University Nijmegen/NIKHEF, Nijmegen, The Netherlands
³⁶Joint Institute for Nuclear Research, Dubna, Russia
³⁷Institute for Theoretical and Experimental Physics, Moscow, Russia
³⁸Moscow State University, Moscow, Russia
³⁹Institute for High Energy Physics, Protvino, Russia
⁴⁰Petersburg Nuclear Physics Institute, St. Petersburg, Russia
⁴¹Lund University, Lund, Sweden,
Royal Institute of Technology and Stockholm University, Stockholm, Sweden,
and Uppsala University, Uppsala, Sweden
⁴²Lancaster University, Lancaster, United Kingdom
⁴³Imperial College, London, United Kingdom
⁴⁴University of Manchester, Manchester, United Kingdom
⁴⁵University of Arizona, Tucson, Arizona 85721, USA
⁴⁶Lawrence Berkeley National Laboratory and University of California, Berkeley, California 94720, USA
⁴⁷California State University, Fresno, California 93740, USA
⁴⁸University of California, Riverside, California 92521, USA
⁴⁹Florida State University, Tallahassee, Florida 32306, USA
⁵⁰Fermi National Accelerator Laboratory, Batavia, Illinois 60510, USA
⁵¹University of Illinois at Chicago, Chicago, Illinois 60607, USA
⁵²Northern Illinois University, DeKalb, Illinois 60115, USA
⁵³Northwestern University, Evanston, Illinois 60208, USA
⁵⁴Indiana University, Bloomington, Indiana 47405, USA
⁵⁵University of Notre Dame, Notre Dame, Indiana 46556, USA
⁵⁶Purdue University Calumet, Hammond, Indiana 46323, USA
⁵⁷Iowa State University, Ames, Iowa 50011, USA
⁵⁸University of Kansas, Lawrence, Kansas 66045, USA
⁵⁹Kansas State University, Manhattan, Kansas 66506, USA
⁶⁰Louisiana Tech University, Ruston, Louisiana 71272, USA
⁶¹University of Maryland, College Park, Maryland 20742, USA
⁶²Boston University, Boston, Massachusetts 02215, USA
⁶³Northeastern University, Boston, Massachusetts 02115, USA
⁶⁴University of Michigan, Ann Arbor, Michigan 48109, USA
⁶⁵Michigan State University, East Lansing, Michigan 48824, USA
⁶⁶University of Mississippi, University, Mississippi 38677, USA
⁶⁷University of Nebraska, Lincoln, Nebraska 68588, USA
⁶⁸Princeton University, Princeton, New Jersey 08544, USA
⁶⁹State University of New York, Buffalo, New York 14260, USA
⁷⁰Columbia University, New York, New York 10027, USA
⁷¹University of Rochester, Rochester, New York 14627, USA
⁷²State University of New York, Stony Brook, New York 11794, USA
⁷³Brookhaven National Laboratory, Upton, New York 11973, USA
⁷⁴Langston University, Langston, Oklahoma 73050, USA
⁷⁵University of Oklahoma, Norman, Oklahoma 73019, USA
⁷⁶Oklahoma State University, Stillwater, Oklahoma 74078, USA
⁷⁷Brown University, Providence, Rhode Island 02912, USA
⁷⁸University of Texas, Arlington, Texas 76019, USA
⁷⁹Southern Methodist University, Dallas, Texas 75275, USA
⁸⁰Rice University, Houston, Texas 77005, USA
⁸¹University of Virginia, Charlottesville, Virginia 22901, USA
⁸²University of Washington, Seattle, Washington 98195, USA
(Received 19 May 2008; published 2 March 2009)

Using approximately 1.3 fb^{-1} of data collected by the D0 detector between 2002 and 2006, we measure the lifetime of the B_c^\pm meson in the $B_c^\pm \rightarrow J/\psi \mu^\pm + X$ final state. A simultaneous unbinned likelihood fit to the $J/\psi + \mu$ invariant mass and lifetime distributions yields a signal of $881 \pm 80(\text{stat})$ candidates and a lifetime measurement of $\tau(B_c^\pm) = 0.448^{+0.038}_{-0.036}(\text{stat}) \pm 0.032(\text{syst}) \text{ ps}$.

One of the most interesting mesons that can be studied at the Tevatron is the B_c^\pm . Unlike most b hadrons, the B_c^\pm meson comprises two heavy quarks (b and c) that can each decay with significant contribution to the decay rate, or they can participate in an annihilation mode. The B_c^\pm meson is therefore predicted [1,2] to have a lifetime of only one-third that of the other B mesons, the shortest of all weakly-decaying b hadrons. Examples of final states where the c quark acts as a spectator while the b quark decays weakly are $B_c^\pm \rightarrow J/\psi \pi^\pm$, $B_c^\pm \rightarrow J/\psi D_s^\pm$, and $B_c^\pm \rightarrow J/\psi \ell^\pm \nu$.

In this Letter we present a measurement of the lifetime of the B_c^\pm meson in the $B_c^\pm \rightarrow J/\psi \mu^\pm + X$ final state with $J/\psi \rightarrow \mu^+ \mu^-$, using approximately 1.3 fb^{-1} [3] of data collected with the D0 detector [4] at the Fermilab Tevatron collider. The detector components most important to this analysis are the central fiber tracker (CFT), the silicon microstrip tracker (SMT), and the muon system [5]. A sample satisfying inclusive muon triggers is used. The invariant mass of the resulting trimuon system is used to help separate the signal and background components and determine their normalizations.

The decay length distribution used to extract the B_c^\pm lifetime is determined from the distance measured for each signal candidate between the reconstructed primary $p\bar{p}$ interaction vertex and the secondary vertex formed by the J/ψ and the third muon. The presence and behavior of the B_c^\pm signal are demonstrated using mass fits following decay length requirements. We construct models of the lifetime distributions of signal and various background components and then perform a simultaneous fit to the trimuon invariant mass and lifetime distributions to measure the lifetime of the B_c^\pm meson.

To simulate B_c^\pm properties in this final state and to determine appropriate selection criteria, Monte Carlo (MC) signal samples of $B_c^\pm \rightarrow J/\psi (\rightarrow \mu^+ \mu^-) \mu^\pm \nu$ are generated using the PYTHIA event generator [6] interfaced with the EVTGEN decay package [7], and followed by full GEANT [8] modeling of the detector response and event reconstruction. For the simulated signal samples, the semi-leptonic decay model of Ref. [9] for B_c^\pm is used. A separate sample using a phase-space decay model is generated for systematic studies. Another possible decay of the B_c^\pm is $B_c^\pm \rightarrow \psi(2S) \mu^\pm + X$ where $\psi(2S) \rightarrow J/\psi \pi^+ \pi^-$, and a sample of this mode is generated as well. To model one of the backgrounds, a large MC sample of inclusive J/ψ events, including b production via gluon splitting ($g \rightarrow b\bar{b}$ where the b and \bar{b} tend to be close in angle rather than back-to-back) and flavor excitation, is used.

We begin by selecting a subsample of events containing at least one $J/\psi \rightarrow \mu^+ \mu^-$ candidate with at least two muons of opposite charge reconstructed in the CFT, SMT, and the muon system. Each muon candidate track must have transverse momentum $p_T > 1.5 \text{ GeV}$, and match hits in the muon system, or it must have $p_T >$

1.0 GeV and an energy deposit in the uranium-liquid-argon calorimeter [4] that is consistent with that of a minimum-ionizing particle.

For at least one of the muons, hits are required in all three layers of the muon detector, and each must have at least two hits in the CFT and at least one hit in the SMT. The signal region is defined in terms of the dimuon mass to be $2.90 < M(\mu^+ \mu^-) < 3.26 \text{ GeV}$. The muon momenta are adjusted according to a mass-constrained fit to the known J/ψ mass [10].

Once a J/ψ is found, an additional third track that can be associated with the J/ψ vertex is sought. The following cuts are applied to the resulting $J/\psi +$ track candidate: the third track must have at least two hits in the SMT, the extrapolation of the three-track momentum must be consistent with coming from the primary vertex, $p_T(\text{third track}) > 3 \text{ GeV}$, $p(\text{third track}) > 4 \text{ GeV}$, $p_T(J/\psi + \text{track}) > 5 \text{ GeV}$, the χ^2 probability to form a common vertex is greater than 1%, the angle between the J/ψ and third track $< 1 \text{ rad}$, and $\cos\theta < 0.99$ where θ is the three-dimensional angle between any two muons. If more than one $J/\psi +$ track candidate is present in an event, the candidate with the lowest χ^2 of the $J/\psi +$ track vertex is selected. The third track must be identified as a muon: it must have hits in all three layers of the muon detector and have timing signals in the muon scintillator detectors consistent within 10 ns of the beam crossing to reduce contamination from cosmic rays. The mass of the $J/\psi + \mu$ candidate is required to be in the range $3 < M(J/\psi \mu) < 10 \text{ GeV}$, resulting in a sample containing 14 753 events.

The invariant mass of the $J/\psi + \mu$ can be used to characterize and separate each of the components that contribute to the $J/\psi + \mu$ candidate sample. There are six contributions (one signal, and five backgrounds): B_c^\pm signal (SI); a real J/ψ associated with a “fake” muon due to a track (JT); fake J/ψ mesons from the combinatorial background (CB); a real muon forming a vertex with a real J/ψ where neither is from a B_c^\pm decay (JM); $B^+ \rightarrow J/\psi K^+$ followed by the decay in flight of $K^+ \rightarrow \mu^+ \nu$; and a $c\bar{c}$ contribution, where a prompt J/ψ is associated with a muon (PR). Each component and its mass parameterization are described below.

The signal mass parameterization is determined from the signal MC sample. Theoretical estimates predict the $B_c^\pm \rightarrow J/\psi \mu^\pm + X$ branching fraction to be approximately 5 to 100 times larger than that of $B_c^\pm \rightarrow \psi(2S) \mu^\pm + X$ [1,11]. This difference gives a 0%–13% feed-down contribution so we assume a 6.5% contribution with a systematic uncertainty of $\pm 6.5\%$.

The invariant mass of the $J/\psi +$ track combinations in data is used to model the JT component. The rate of what are denoted fake muons is small and primarily due to decays in flight of $\pi^\pm \rightarrow \mu^\pm \nu$ and $K^\pm \rightarrow \mu^\pm \nu$. The $B^+ \rightarrow J/\psi K^+$ decay is used to measure the contribution

of this component. Fits are made to the B^+ mass peak in the $J/\psi + \mu$ sample and the $J/\psi + \text{track}$ sample, and the ratio of the number of B^+ events in the two samples is taken as the fraction of events that are due to a real J/ψ but a fake μ . Contributions due to $B^+ \rightarrow J/\psi \pi^+$ or $B_c^+ \rightarrow J/\psi \pi^+$ are estimated to be negligible.

To describe the CB component, a normalized mass parameterization is formed from events in the J/ψ mass sidebands. The sideband regions are defined to be events with $M(\mu^+ \mu^-)$ in the range 2.62–2.80 GeV or 3.40–3.58 GeV. The normalization is taken from the fitted number of background events in the signal region under the J/ψ mass peak.

The JM component represents a significant background that is dominated by $b\bar{b}$ backgrounds, where one long-lived b hadron decays to $J/\psi + X$ and the other decays semileptonically to a muon (or via a cascade decay $b \rightarrow c \rightarrow \mu$). The requirement that the J/ψ and μ be close in angle increases the acceptance for $b\bar{b}$ production via gluon splitting relative to $q\bar{q}$ or $gg \rightarrow b\bar{b}$. To model this background, the J/ψ QCD MC sample is used with the requirement that the parent of the J/ψ does not arise from a prompt B_c^\pm meson, B^\pm , or $c\bar{c}$ (the latter two components are estimated using the data and described below).

For the B^+ component, a fit is made to the mass peak of the B^+ in the $J/\psi + \mu$ data sample. This fitted distribution is then used as a mass parameterization for the B^+ component, thus reducing the uncertainty in the modeling of the width of the mass peak.

The transverse decay length L_{xy} is defined as the displacement of the $J/\psi + \mu$ vertex from the primary vertex [12] projected onto the direction of the transverse momentum vector of the $J/\psi + \mu$ system, signed by the dot product of the two vectors. Candidates with $L_{xy} < 0$ are used to estimate the mass parameterization of the PR component.

To check the validity of the modeling of the $M(J/\psi \mu)$ distribution, a fit is first made on the mass distribution of the $J/\psi + \mu$ sample using the parameterizations of the six contributions described above. Separate fits are made as the requirement on L_{xy} is raised to increasingly suppress the background. Good agreement of the fitted mass components is observed at all L_{xy} values. To further check for the presence of the B_c^\pm signal, a requirement is placed on the transverse decay length significance: $L_{xy}/\sigma(L_{xy}) > 4$, where $\sigma(L_{xy})$ is the uncertainty on L_{xy} . Figure 1 shows the fit to the mass distribution after subtracting the J/ψ sideband and B^+ components. In this sample, the statistical significance of the B_c^\pm signal component is 6.4σ .

The lifetime of the B_c^\pm , τ , is related to the transverse decay length by $L_{xy} = c\tau \frac{p_T(B_c^\pm)}{m(B_c^\pm)}$, where p_T and m are the transverse momentum and rest mass of the B_c^\pm , respectively. When the B_c^\pm meson decays semileptonically, it cannot be fully reconstructed due to the escaping neutrino, and thus $p_T(B_c^\pm)$ cannot be determined. The p_T of the

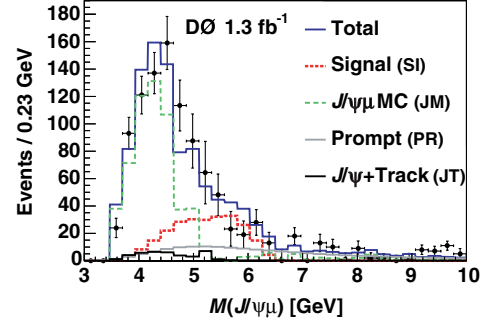


FIG. 1 (color online). Fit to the mass of the $J/\psi + \mu$ vertex with J/ψ mass sideband (CB) and B^+ components subtracted and decay length significance $L_{xy}/\sigma(L_{xy}) > 4$ required.

$J/\psi + \mu$ system is used instead as an approximation. A correction factor, $K = p_T(J/\psi \mu)/p_T(B_c^\pm)$, determined using signal MC calculations, is introduced to estimate $p_T(B_c^\pm)$. To obtain the B_c^\pm lifetime, the visible-proper decay length (VPDL) is measured, defined as $L_{xy} \frac{m(B_c^\pm)}{p_T(J/\psi \mu)} = \frac{c\tau}{K}$.

The K -factor distribution is applied statistically by smearing the exponential decay distribution when extracting $c\tau(B_c^\pm)$ from the VPDL distribution in the lifetime fit. The mass of the B_c^\pm is taken from [13]. To take advantage of events with better resolution, the K factor is applied in the analysis in six bins of $M(J/\psi \mu)$.

An unbinned likelihood fit is used to measure the average lifetime, maximizing \mathcal{L} over all i candidates, where

$$\begin{aligned} \mathcal{L} = & \prod_i [f_{JT} \mathcal{F}_{JT}^i + (1 - f_{JT})(f_{CB} \mathcal{F}_{CB}^i + (1 - f_{CB}) \\ & \times \{f_{SI} \mathcal{F}_{SI}^i + f_{JM} \mathcal{F}_{JM}^i + f_{B^+} \mathcal{F}_{B^+}^i \\ & + (1 - f_{SI} - f_{JM} - f_{B^+}) \mathcal{F}_{PR}^i\})]. \end{aligned} \quad (1)$$

Each component \mathcal{F} consists of a combination of a mass-shape parameterization and a lifetime functional model, each described below, to allow for a simultaneous fit of the fraction components and $\tau(B_c^\pm)$. The fractions f of each component have been described earlier. The fraction $f_{JT} = 0.034 \pm 0.002$ is taken from fits to the B^+ peak and $f_{CB} = 0.667 \pm 0.004$, is found from J/ψ mass sideband fits. The lifetime component of \mathcal{F}_{SI} is an exponential function with decay constant proportional to $\tau(B_c)$ convoluted with a Gaussian resolution function and smeared with normalized K -factor distributions. The width of the Gaussian resolution function uses the event-by-event uncertainty $\sigma(\lambda_i)$ on the VPDL, multiplied by a floating scale factor s to take into account any systematic underestimate of $\sigma(\lambda_i)$ due to tracking systematic uncertainties. A double Gaussian function, centered at VPDL = 0, is used to model \mathcal{F}_{PR} . The width of the inner Gaussian is given by $s \cdot \sigma(\lambda_i)$, and the multiplicative factor for the width of the outer Gaussian is determined using MC samples and data candidates with negative decay length. Fits are made to the respective

VPDL distributions to obtain \mathcal{F}_{JT} and \mathcal{F}_{CB} . Empirical functional forms are used for both as fixed shapes, and the normalizations via the fractions f_{JT} and f_{CB} are allowed to float in the fit within Gaussian constraints given by their uncertainties. The \mathcal{F}_{JM} term consists of a negative-slope exponential and two positive-slope exponentials. The normalization of the negative-slope exponential, along with the normalization and slope of one of the positive-slope exponentials are constrained by the values estimated in the inclusive J/ψ MC sample. The slope of the negative-slope and second positive-slope exponential are allowed to float in the final fit. \mathcal{F}_{B^+} is a single exponential function with the slope constrained to the world-average value [10] convolved with the same Gaussian resolution function as for the signal lifetime model.

Before examining the fit to the data, possible lifetime biases are studied. Signal MC samples mixed with background are generated with different lifetimes. Fits to these samples and ensemble tests indicate no significant bias and demonstrate the validity of the extracted statistical uncertainty.

A simultaneous fit to the $(J/\psi\mu)$ invariant mass and VPDL distributions is performed using all the components described above. The fitted lifetime of the B_c^\pm meson is found to be $\tau(B_c^\pm) = 0.448_{-0.036}^{+0.038}(\text{stat})$ with an estimated signal sample of $881 \pm 80(\text{stat})$ candidates. The fitted value of the scale factor is $s = 1.35 \pm 0.02$. Figure 2 shows the VPDL distribution of the $J/\psi + \mu$ sample with projections of the fit result overlaid.

Stability checks made by dividing the data in half based on various selections show no significant lifetime variations. The systematic uncertainties considered are discussed in detail below and are summarized in Table I.

Variations of the B_c^\pm mass within its measurement uncertainties [13] make a negligible difference in the lifetime. The B_c^\pm signal modeling uncertainty is estimated from the difference between the Ref. [9] model and phase-space decay model. The uncertainty in $p_T(B_c^\pm)$ is found by reweighting the spectrum to correspond to varying the factorization and renormalization scales $\mu_F = \mu_R =$

$\sqrt{p_T^2(b) + m_b^2}$ by factors of a half and two [14]. To address uncertainties on the predicted $p_T(b)$ for the signal and background component distributions, a momentum weighting factor that is applied to MC samples to improve the simulation and include the effects of the triggers is removed. In all of the above cases, both new signal mass parameterizations and K -factor distributions are generated and the analysis repeated. To assess the systematic uncertainty due to the modeling of the inclusive J/ψ MC mass distribution, contributions due to $b\bar{b}$ production via gluon splitting and then flavor excitation are entirely removed. The shape of the mass parameterization for the prompt component is varied within the statistical errors of its determination, and the observed lifetime variation assigned as a systematic error. All of the systematic uncertainties described above are added in quadrature and summarized in Table I under the category of mass model uncertainties.

To test the assumption that the modeling of the lifetime of the J/ψ combinatoric background can be approximated by taking the average of the upper and lower mass sidebands, the fit is performed using only the high or the low mass sideband, and a systematic uncertainty of one half the resulting shifts in lifetime is assigned. The scale factor s is varied over the range of values, 1.2–1.4, observed in other lifetime analyses [15] as well as assigned a functional form and the variation in lifetime assigned as a systematic uncertainty. In the prompt lifetime model, a single Gaussian function instead of a double Gaussian is used. The shape parameters of the sideband lifetime model are changed by varying the fit parameters within their uncertainties. The parameters defining the J/ψ QCD MC lifetime model are varied around their central values by $\pm 1\sigma$. For the B^+ lifetime model, the central value is changed by $\pm 1\sigma$. The B^+ lifetime is also allowed to float as a systematic study on the B_c^\pm lifetime as well as a check of the B^+ lifetime, finding a value of 1.88 ± 0.19 ps, consistent with the world-average value of 1.638 ± 0.011 ps [10]. All of the systematic uncertainties described above are added in quadrature under the category of lifetime model uncertainties.

Smaller systematic uncertainties arise from the variation of the fraction of the feed-down $B_c \rightarrow \psi(2S)X$ signal component between 0% and 13%, and from possible alignment effects, estimated using signal MC calculations with

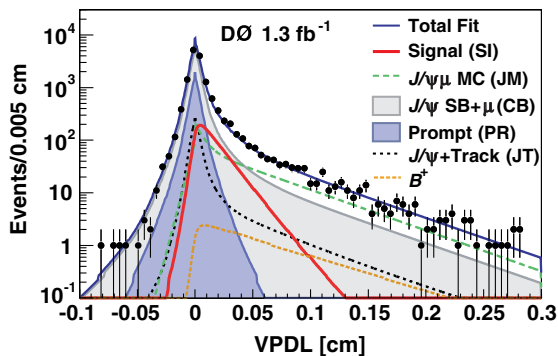


FIG. 2 (color online). VPDL distribution of the $J/\psi\mu$ sample with the projected components of the fit overlaid.

TABLE I. Summary of estimated systematic uncertainties.

Systematic source	$\Delta\tau$ (ps)
Mass model uncertainty	± 0.021
Lifetime model uncertainty	± 0.022
Signal feed-down fraction	± 0.005
Alignment	± 0.006
Total	± 0.032

a modified detector geometry within the alignment tolerances.

In summary, using approximately 1.3 fb^{-1} of data, the lifetime of the B_c^\pm meson is measured in the $B_c^\pm \rightarrow J/\psi \mu^\pm + X$ final state. Using an unbinned likelihood simultaneous fit to the $J/\psi + \mu$ invariant mass and lifetime distributions we measure

$$\tau(B_c^\pm) = 0.448_{-0.036}^{+0.038}(\text{stat}) \pm 0.032(\text{syst}) \text{ ps.}$$

This measurement is consistent with theoretical predictions of $0.55 \pm 0.15 \text{ ps}$ in an operator product expansion calculation [1] and $0.48 \pm 0.05 \text{ ps}$ using QCD sum rules [2]. It is also consistent with, but more precise than, the most recent result from the CDF collaboration [16], $\tau(B_c) = 0.463_{-0.065}^{+0.073} \pm 0.036 \text{ ps}$ [16], and hence is the most precise measurement of $\tau(B_c^\pm)$ to date.

We thank the staffs at Fermilab and collaborating institutions, and acknowledge support from the DOE and NSF (USA); CEA and CNRS/IN2P3 (France); FASI, Rosatom and RFBR (Russia); CNPq, FAPERJ, FAPESP and FUNDUNESP (Brazil); DAE and DST (India); Colciencias (Colombia); CONACyT (Mexico); KRF and KOSEF (Korea); CONICET and UBACyT (Argentina); FOM (The Netherlands); STFC (United Kingdom); MSMT and GACR (Czech Republic); CRC Program, CFI, NSERC and WestGrid Project (Canada); BMBF and DFG (Germany); SFI (Ireland); The Swedish Research Council (Sweden); CAS and CNSF (China); and the Alexander von Humboldt Foundation.

*Visitor from Augustana College, Sioux Falls, SD, USA.

†Visitor from The University of Liverpool, Liverpool, UK.

‡Visitor from ICN-UNAM, Mexico City, Mexico.

§Visitor from II. Physikalisches Institut, Georg-August-University, Göttingen, Germany.

||Visitor from Helsinki Institute of Physics, Helsinki, Finland.

¶Visitor from Universität Zürich, Zürich, Switzerland.

**Deceased

- [1] V. V. Kiselev, A. E. Kovalsky, and A. K. Likhoded, Nucl. Phys. B **585**, 353 (2000).
- [2] V. Kiselev, arXiv:hep-ph/0308214, and references therein.
- [3] T. Andeen *et al.*, Report No. FERMILAB-TM-2365, 2007.
- [4] V. M. Abazov *et al.* (D0 Collaboration), Nucl. Instrum. Methods Phys. Res., Sect. A **565**, 463 (2006).
- [5] V. M. Abazov *et al.*, Nucl. Instrum. Methods Phys. Res., Sect. A **552**, 372 (2005).
- [6] T. Sjöstrand *et al.*, Comput. Phys. Commun. **135**, 238 (2001).
- [7] D. J. Lange, Nucl. Instrum. Methods Phys. Res., Sect. A **462**, 152 (2001).
- [8] R. Brun and F. Carminati, CERN Program Library Long Writeup Report No. W5013, 1993 (unpublished).
- [9] D. Scora and N. Isgur, Phys. Rev. D **52**, 2783 (1995).
- [10] C. Amsler *et al.*, Phys. Lett. B **667**, 1 (2008).
- [11] D. Ebert *et al.*, Phys. Rev. D **68**, 094020 (2003), and references therein.
- [12] J. Abdallah *et al.* (DELPHI Collaboration), Eur. Phys. J. C **32**, 185 (2004).
- [13] A. Abulencia *et al.* (CDF Collaboration), Phys. Rev. Lett. **96**, 082002 (2006).
- [14] K. M. Cheung and T. C. Yuan, Phys. Rev. D **53**, 1232 (1996).
- [15] V. M. Abazov *et al.* (D0 Collaboration), Phys. Rev. Lett. **99**, 142001 (2007); **99**, 182001 (2007).
- [16] A. Abulencia *et al.* (CDF Collaboration), Phys. Rev. Lett. **97**, 012002 (2006).